Imaging the dust and the gas around Mira using ALMA and SPHERE/ZIMPOL

Theo Khouri[1], Wouter H. T. Vlemmings[1], Hans Olofsson[1], Christian Ginski[2], Elvire De Beck[1], Matthias Maercker[1] and Sofia Ramstedt[3]

[1]Department of Space, Earth and Environment, Chalmers University of Technology, Onsala Space Observatory, 439 92 Onsala, Sweden
email: theokhouri@gmail.com

[2]Sterrewacht Leiden, P.O. Box 9513, Niels Bohrweg 2, 2300RA Leiden, The Netherlands

[3]Department of Physics and Astronomy, Uppsala University, Box 516, 751 20, Uppsala, Sweden

Abstract. The mass-loss mechanism of asymptotic giant branch stars has long been thought to rely on two processes: stellar pulsations and dust formation. The details of the mass-loss mechanism have remained elusive, however, because of the overall complexity of the dust formation process in the very dynamical pulsation-enhanced atmosphere. Recently, our understanding of AGB stars and the associated mass loss has evolved significantly, thanks both to new instruments which allow sensitive and high-angular-resolution observations and the development of models for the convective AGB envelopes and the dust formation process. ALMA and SPHERE/ZIMPOL on the VLT have been very important instruments in driving this advance in the last few years by providing high-angular resolution images in the sub-mm and visible wavelengths, respectively. I will present observations obtained using these instruments at the same epoch (2.5 weeks apart) of the AGB star Mira that resolve even the stellar disk. The ALMA data reveals the distribution and dynamics of the gas around the star, while the polarised light imaged using SPHERE shows the distribution of the dust grains expected to drive the outflows. Moreover, the observations show a central source surrounded by asymmetric distributions of gas and dust, with complementary structures seen in the two components. We model the observed CO $v = 1$, $J = 3 - 2$ line to determine the density, temperature and velocity of gas close to the star. This model is then used to estimate the abundance of AlO. Our results show that only a very small fraction of aluminium ($\lesssim 0.1\%$) is locked in AlO molecules. We also calculate models to fit the observed polarised light based on the gas densities we find. The low level of visible-light polarisation detected using ZIMPOL implies that, at the time of the observations, aluminium atoms are either not efficiently depleted into dust or the aluminium-oxide grains are relatively small ($\lesssim 0.02$ μm).

1. Introduction

At the end of their lives, low- and intermediate-mass stars evolve through the asymptotic giant branch (AGB) phase. In the AGB, these stars return a large fraction of their initial mass to the interstellar medium through slow ($v_\infty \sim 10$ km/s) but massive (10^{-8} M$_\odot$/yr $\lesssim \dot{M} \lesssim 10^{-4}$ M$_\odot$/yr) outflows. The wind-driving mechanism is thought to consist of a two-step process. First, large convective cells and stellar pulsations lift material up to distances where the temperatures are low enough for dust condensation to happen. Then, radiation pressure acting on the newly-formed dust grains leads to an outflow (Höfner & Olofsson 2018). Predicting the mass-loss rate of a given star

31
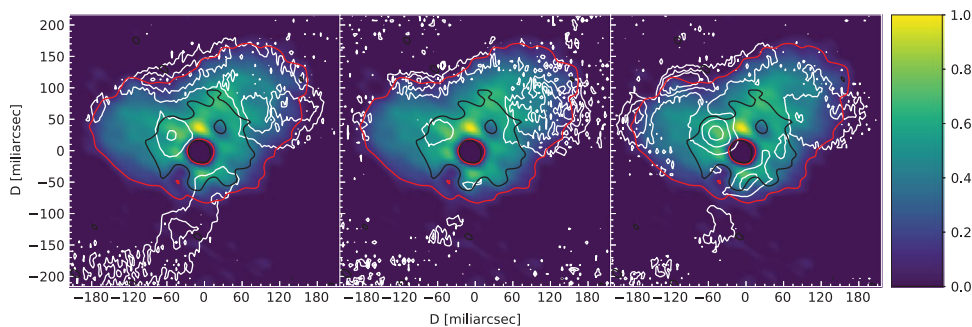
Figure 1. The colour scale shows the normalised emission in the SO $N_J = 8_8 - 7_7$ line imaged using ALMA and the white contours show the polarisation degree observed using SPHERE with three filters (*left*: 0.65 μm, *middle*: 0.75 μm, and *right*: 0.82 μm). The contours show the 1.5, 2.5, and 3.5% levels. The ALMA image is normalised to its peak value. The red and black lines marks the 10%-level contour of the SO $N_J = 8_8 - 7_7$ and CO $v = 1, J = 3 - 2$ emission lines, respectively. The contour of the SO line shows the boundary of the high-gas-density region detected by ALMA. The accumulation of dust along the edge of this high-gas-density region is particularly seen between the north and west directions. Absorption against the star is seen as negative fluxes in the centre of these stellar-continuum-subtracted images.

is not yet possible at present, because the modelling of convection is difficult and the stellar-pulsation mechanism and the details of the dust formation process are still not understood.

For stars richer in oxygen than carbon (O-rich), the outflows are thought to be driven by *scattering* of radiation off dust grains. This is only possible if the dust grains grow to relatively large sizes, ~ 0.3 μm in radius (Höfner 2008). Observations revealed polarised light produced by scattering of radiation off dust grains with sizes within the required range (Norris *et al.* 2012). SPHERE/ZIMPOL observations now allow for studies of the distribution and amount of such large grains around several O-rich AGB stars (Khouri *et al.* 2016; Ohnaka *et al.* 2017). For the closer-by sources, the dust-formation region, and even the stellar disc, is clearly resolved (see Fig. 1). The dust condensation sequence is not well understood but the current picture is that aluminium oxide grains from close to O-rich AGB stars (Gobrecht *et al.* 2016) and that iron-free silicates condensate at slightly larger radii on top of the aluminium-oxide seeds. The aluminium-oxide grains are expected to grow to relative large sizes (~ 0.3 μm) and have large scattering cross-sections at visible wavelengths (Höfner *et al.* 2016). The dust mass of aluminium oxide grains is expected to be too low for driving the outflow, however, because of the low abundance of aluminium (Bladh & Höfner 2012). To study the dust-formation and wind-driving mechanisms, we observed the O-rich AGB stars Mira using SPHERE/ZIMPOL and ALMA. The work discussed here is present in more depth in Khouri *et al.* (submitted).

At 107 parsecs, Mira is the archetypal object of the class of Mira variables. Mira has a companion (thought to be a white dwarf) with an orbital separation of ~ 90 AU and a projected distance of 0.5 arcseconds (e.g., Ireland *et al.* 2007). Mira B is not expected to have a significant gravitational effect on material in the wind-acceleration region (at distance $\lesssim 10$ AU from Mira A, e.g., (Mohamed & Podsiadlowski 2012).

2. Observations

ZIMPOL observations of Mira were acquired using filters NR, cnt748, and cnt820 on 27 November 2017 (ESO program ID 0100.D-0737, PI: Khouri). The ALMA observations were obtained 18 days before the ZIMPOL observations on 9 November 2017

(project 2017.1.00191.S, PI: Khouri). The data were acquired at post-minimum light phase ($\varphi \approx 0.7$) of Mira A. The data reduction followed standard procedures for both instruments (Khouri *et al.*, submitted).

The ZIMPOL data reveal dust grains around Mira A, but also around Mira B and in a dusty trail that connects the two stars. Within an aperture with radius of 80 mas around Mira A, we find a polarisation degree of at most $\sim 2\%$ (see discussion in Khouri *et al.*, submitted). The degree of polarisation measured around Mira A peaks at $\approx 3.2\,\%$ in NR, $\approx 3.5\,\%$ in cnt748 and $\approx 4.0\,\%$ in cnt820, being is relatively lower than what is seen for other close-by O-rich AGB stars, such as R Dor (Khouri *et al.* 2016), W Hya (Ohnaka *et al.* 2017), and R Leo (archival data). The polarization degree around these other AGB stars peaks at $> 7\%$ and is particular high ($> 10\%$) close to minimum-light phase.

In the reduced ALMA data, we obtained a root-mean squared (rms) noise of ~ 1.4 mJy for a spectral resolution of ~ 1.7 km s^{-1}. The continuum images have an rms noise of 0.4 mJy/beam and the continuum flux density of Mira A is measured to be 250.6 ± 0.2 mJy. The ALMA observations reveal more than one hundred spectral lines in the observed spectral windows, 329.25 – 331.1 GHz, 331.1 – 333.0 GHz, 341.35 – 343.25, and 343.2 – 345.1 GHz.

A well-define emission region (see Fig. 1) is seen in low-excitation lines of several species, such as SO, ^{13}CO, SO$_2$, and to a lesser degree AlO and PO. We interpret this region to be delimited by a steep density decline at its outer edge. Interestingly, the polarization degree measured using ZIMPOL show peaks that follow the edge of this molecular-line emission region, especially in the north and northeast regions (see Fig. 1). The cause for both this well-defined molecular-line emission region and the apparent accumulation of dust at its outer edge is not obvious from our data. We speculate that a recent increase in the mass-loss rate could have led to higher densities close to the star. The mass-loss rate burst could be connected to a recent X-ray outburst observed towards Mira A in 2003 (Karovska *et al.* 2005). As pointed out by the authors, such an X-ray burst could have significant consequences for the mass-loss rate of Mira A. The edge of the molecular-line emission region we see is at a distance of ~ 18 au of the star. Therefore, gas would need to travel at a speed of ~ 6 km/s to cover this distance over the period of 14 years separating the observations reported by us from those by Karovska *et al.* Monitoring the evolution of the molecular-line emission region will help determine whether this scenario is correct.

3. Models

To study the distributions of gas and dust close to Mira A, we calculated radiative-transfer models to fit both the emission in the line CO $v = 1, J = 3 - 2$ and the polarization degree observed in the same region around Mira A. The CO $v = 1, J = 3 - 2$ line is expected to be only excited in the high-density extended atmospheres and close environment of AGB stars and is a good tracer of gas in this region (e.g., Vlemmings *et al.* 2017). The details of the fitting procedure are given in Khouri *et al.* (submitted). Below, we summarise the main findings.

Our best if model to the CO $v = 1, J = 3 - 2$ is shown in Fig. 2. Our results implie a gas mass in the region traced by the vibrationally-excited CO line of $(3.8 \pm 1.3) \times 10^{-4} M_{\odot}$. A comparison of the prediction from our best models to the observed ^{13}CO line in this inner region suggests that models with gas masses in the lower end of our uncertainty interval are preferred. For these calculations, we assumed a ^{12}C-to-^{13}C ratio of 10 ± 3 (Hinkle *et al.* 2016).

We used this model to constrain the abundance of AlO and we find that only $\sim 0.1\%$ of the aluminium atoms are accounted for by AlO molecules, assuming solar composition
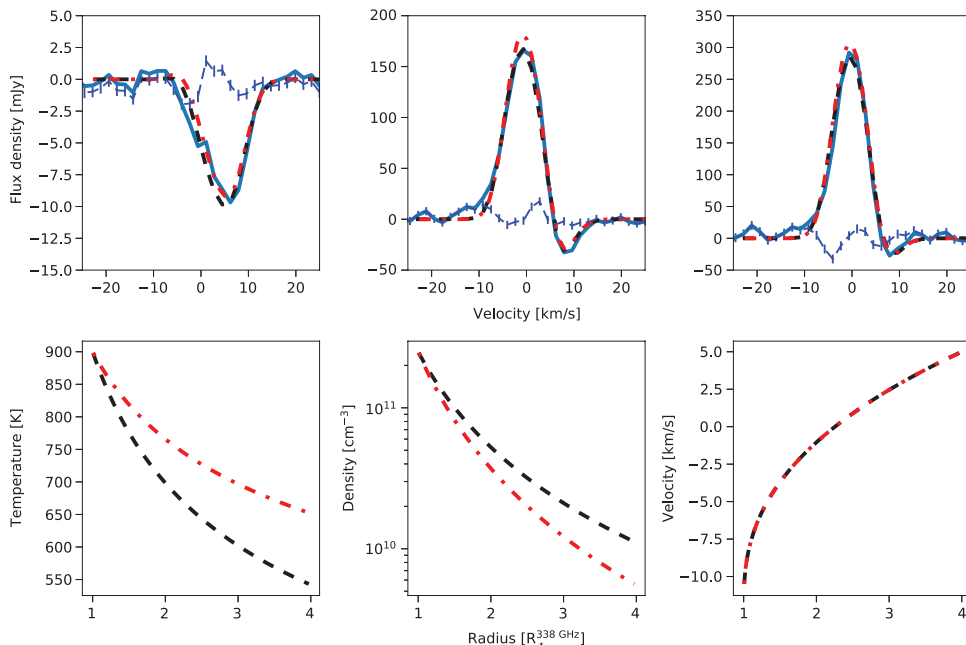
Figure 2. Models for the CO $v = 1, J = 3 - 2$ line emission. The black dashed line shows the best-fitting model and the dashed red line shows the preferred model when the $^{13}CO\ J = 3 - 2$ line is also considered. *Upper panels:* Best model fits to the observed CO $v = 1, J = 3 - 2$ line (solid blue line) extracted using apertures of 20, 50, and 100 mas, from left to right. The thin, dashed blue line shows the residuals with errorbars. *Lower panels:* temperature, density and velocity profiles of the best-fit and preferred models.

(Asplund *et al.* 2009). Hence, there is ample room for aluminium condensation into aluminium oxide grains as expected to happen close to O-rich AGB stars from observations (e.g., Zhao-Geisler *et al.* 2011; Karovicova *et al.* 2013; Khouri *et al.* 2015) and supported by theoretical calculations (Gobrecht *et al.* 2016; Höfner *et al.* 2016). We note that a definitive answer on the amount of aluminium depletion cannot be obtained based on this data because the abundance of other aluminium-bearing molecules was not determined. Nonetheless, studies that have target molecules that could account for a significant fraction of aluminium atoms have not found any species that appears to have significantly higher abundance than AlO (e.g., Kamiński *et al.* 2016; Decin *et al.* 2017).

We used the radiative transfer code MCMax (Min *et al.* 2009) to calculate the polarisation degree from models with aluminium oxide dust grains. The density profile of the dust was derived from the gas density profile in our best-fitting models and scaled assuming different aluminium depletion levels. We calculated the opacities using data from different authors for aluminium oxide grains (Suh 2016; Koike *et al.* 1995; Harman *et al.* 1994; Edlou *et al.* 1993) and a hollow-spheres grain model (Min *et al.* 2003). We considered a single grain size for each model calculation, varying it between 0.01 and 1.0 μm. We find that the models reproduce the low level of visible-light polarisation in the vibrationally-excited CO region only if the grains are very small (sizes $\lesssim 0.02\ \mu$m) or account for a small fraction of aluminium atoms ($\sim 1\%$ for 0.3 μm grains).

References

Asplund, M., Grevesse, N., Sauval, A. J., & Scott, P. 2009, *ARAA*, 47, 481
Bladh, S. & Höfner, S. 2012, *A&A*, 546, A76

Decin, L., Richards, A. M. S., Waters, L. B. F. M., *et al.* 2017, *A&A*, 608, A55

Edlou, S. M., Smajkiewicz, A., & Al-Jumaily, G. A. 1993, *Applied Optics*, 32, 5601

Gobrecht, D., Cherchneff, I., Sarangi, A., Plane, J. M. C., & Bromley, S. T. 2016, *A&A*, 585, A6

Harman, A. K., Ninomiya, S., & Adachi, S. 1994, *Journal of Applied Physics*, 76, 8032

Hinkle, K. H., Lebzelter, T., & Straniero, O. 2016, *ApJ*, 825, 38

Höfner, S. 2008, *A&A*, 491, L1

Höfner, S., Bladh, S., Aringer, B., & Ahuja, R. 2016, *A&A*, 594, A108

Höfner, S. & Olofsson, H. 2018, *AAR*, 26, 1

Ireland, M. J., Monnier, J. D., Tuthill, P. G., *et al.* 2007, *ApJ*, 662, 651

Kamiński, T., Wong, K. T., Schmidt, M. R., *et al.* 2016, *A&A*, 592, A42

Karovicova, I., Wittkowski, M., Ohnaka, K., *et al.* 2013, *A&A*, 560, A75

Karovska, M., Schlegel, E., Hack, W., Raymond, J. C., & Wood, B. E. 2005, *ApJ* (Letters), 623, L137

Khouri, T., Maercker, M., Waters, L. B. F. M., *et al.* 2016, *A&A*, 591, A70

Khouri, T., Waters, L. B. F. M., de Koter, A., *et al.* 2015, *A&A*, 577, A114

Koike, C., Kaito, C., Yamamoto, T., *et al.* 1995, *Icarus*, 114, 203

Min, M., Dullemond, C. P., Dominik, C., de Koter, A., & Hovenier, J. W. 2009, *A&A*, 497, 155

Min, M., Hovenier, J. W., & de Koter, A. 2003, *A&A*, 404, 35

Mohamed, S., & Podsiadlowski, P. 2012, *Balt. Ast.*, 21, 88

Norris, B. R. M., Tuthill, P. G., Ireland, M. J., *et al.* 2012, *Nature*, 484, 220

Ohnaka, K., Weigelt, G., & Hofmann, K.-H. 2017, *A&A*, 597, A20

Suh, K.-W. 2016, *Journal of Korean Astronomical Society*, 49, 127

Vlemmings, W., Khouri, T., O'Gorman, E., *et al.* 2017, *Nat. Ast.*, 1, 848

Zhao-Geisler, R., Quirrenbach, A., Köhler, R., Lopez, B., & Leinert, C. 2011, *A&A*, 530, A120

Discussion

LILJEGREN: Would your results for the grain size change if you considered grains consisting of an aluminium-oxide core with silicate mantle?

KHOURI: I think that would make it worse, actually, since in that case aluminium atoms would account for a relatively smaller mass fraction of the grains. Considering that the scattering properties of silicates are not too different from those of aluminium oxide, I would expect a stronger polarization signal for the same amount of aluminium depletion for core-mantle grains.

SCICLUNA: You can also constrain the grain sizes based on the spectral dependence of the polarized light, right? Why haven't you tried that?

KHOURI: Our observations were affected by the beam-shift effect of ZIMPOL, which makes the polarized light close to the star somewhat uncertain. Since the levels of polarization degree were already relatively low, we choose to consider an upper limit on the polarization degree and calculate the expected level of polarization for different assumed grain sizes and depletion factors.